

Comparative performance evaluation of carbon dot-based paper immunoassay on Whatman filter paper and nitrocellulose paper in the detection of HIV infection

Aditya Kurdekar¹ · L. A. Avinash Chunduri¹ · Eswarappa Pradeep Bulagonda² ·
Mohan Kumar Haleyrigisetty³ · Venkataramaniah Kamiseti¹ · Indira K. Hewlett³

Received: 15 April 2016 / Accepted: 11 June 2016 / Published online: 22 June 2016
© Springer-Verlag Berlin Heidelberg 2016

Abstract Carbon dots synthesized from citric acid and ethylene diamine by a one-step hydrothermal technique were used to develop a carbon dot-based paper immunoassay (CDPIA) for rapid detection of HIV-1 p24 antigen. In the present study, the 96-well template was hand patterned using a wax pencil, as a prototype method, on two types of paper, (1) Whatman filter paper and (2) nitrocellulose paper. The sandwich immunoassay was performed on both paper microplates for detection of HIV-1 p24 antigen which is an early marker of HIV infection. The detection range was from 10 $\mu\text{g/mL}$ to 1 ng/mL for the Whatman filter paper while the nitrocellulose paper exhibited a higher range from 10 $\mu\text{g/mL}$ to 250 pg/mL . CDPIA on the nitrocellulose paper (CDNIA) exhibited a fourfold increase in sensitivity and reduced the assay time by threefold compared with CDPIA on Whatman paper (CDWIA). HIV-negative and HIV-positive plasma samples were tested using CDNIA for the presence of HIV-1 p24 antigen. This immunoassay exhibited no false-positive and false-negative results with the clinical samples tested. This simple

and sensitive paper-based HIV-1 p24 antigen assay may be useful in preventing HIV transmission by blood transfusion in resource-limited settings by reducing the antibody negative, infectious window period in blood donors and for early diagnosis of HIV infected individuals where nucleic acid-based testing is not practical or feasible.

1 Introduction

Infectious diseases are the major causes of death in children and one of the leading causes of deaths in adults (Infectious diseases 2016). Although a wide range of diseases such as malaria, tuberculosis, respiratory infections prevail, a major disease which has alarmed the world is the acquired immune deficiency syndrome (AIDS) caused by human immunodeficiency virus (HIV) which has globally infected 36.9 million people and does not have a cure (AIDS GLOBAL STATISTICS 2015). While antiretroviral therapies (ART) are available which can prolong life and also improve the quality of life by helping affected individuals to manage the disease, it still does not offer a complete recovery or cure (Moore and Chaisson 1999). Moreover, the situation is aggravated further in developing countries which have limited access to resources where ART cannot be provided. Thus, there is a very strong emphasis on the need for better diagnostic techniques for early detection of this disease which can prevent its further transmission to healthy, at-risk individuals. This highlights the need for efficient, ultrasensitive and inexpensive diagnostic kits easily deployable in any part of the world.

Enzyme-linked immunosorbent assay (ELISA) is the most commonly used detection technique for various biomolecules and pathogens (Lequin 2005). Due to its sensitivity and widespread application, it is widely used for HIV

Disclaimer: The findings and conclusions in this report are those of the authors and do not necessarily represent the views of the Food and Drug Administration, U.S. Department of Health and Human Services.

✉ Venkataramaniah Kamiseti
vrkamiseti@gmail.com

¹ Department of Physics, Sri Sathya Sai Institute of Higher Learning, Prasanthi Nilayam, Puttaparthi 515134, India

² Department of Biosciences, Sri Sathya Sai Institute of Higher Learning, Prasanthi Nilayam, Puttaparthi 515134, India

³ Laboratory of Molecular Virology, Center for Biologics Evaluation and Research (CBER), Food and Drug Administration, Silver Spring, MD 2099, USA

detection. Current diagnostic tools detect up to 15 pg/mL and 0.5 pg/mL by conventional ELISA and TSA-mediated signal amplification-boosted ELISA, respectively (Tang and Hewlett 2010; Schüpbach et al. 1996; Sutthent et al. 2003). While these conventional ELISA detection protocols with greater than 99 % sensitivity are already in use, they are suboptimal because it takes up to 3 months for the antibodies to become detectable in the plasma (Anderson et al. 1986; Sherman et al. 2005). This problem can be tackled by targeting the HIV-1 capsid protein, p24 antigen, which has been reported to be measurable in blood immediately after infection (Fiebig et al. 2003). Moreover, the cost, assay duration and infrastructural requirements reduce the applicability of conventional ELISA in resource-limited settings. These drawbacks have called for a detection system which is quick and efficient and at the same time inexpensive. One promising candidate for such a platform is paper. Paper-based immunoassays for biological detection are important because of following features of paper: (i) it is inexpensive, easy to handle and store; (ii) it has a very high absorption capacity for biomolecules; (iii) it is made of cellulose or cellulose-based polymers which makes it biocompatible (Pelton 2009); (iv) biomolecules can be added by chemically modifying the structure of the paper by adding functional groups (Zhao et al. 2008); (v) it can be easily disposed by incarceration (Martinez et al. 2010); and (vi) paper can be easily printed upon making it easier to fabricate devices (Lab on paper 2008). Hence, paper-based platforms are an optimal choice for an efficient point-of-care (POC) diagnostic tool in a resource-limited setting.

Although most paper immunoassays use chromogenic (absorbance-based) reporters which generate a coloured product which is visible to the naked eye (Ellerbee et al. 2009), it is advantageous to use fluorescent reporters which generate fluorescence as the detection signal. While the chromogenic methods may be reliable and significantly reduce the cost as the chromogenic change can be read with naked eyes, fluorescence detection techniques are 1000 times more sensitive than absorbance-based techniques (Bartlett and Entzeroth 2006). Also in case of a quantitative measurement of the target molecule, fluorescence detection methods are more reliable than chromogenic methods as they provide 80-fold higher dynamic range for a given sample (Which Western Blot Detection Method Should You Use? 2012). The reporting agent in fluorescent-based techniques is fluorescent molecules or fluorophores. While a wide range of fluorophores have been used in immunoassays, they have not been explored extensively with paper as the substrate. These fluorophores are generally organic fluorophores which have high quantum yield and are commercially available (Resch-Genger et al. 2008), and heavy metal-doped semiconductor nanocrystals which have easy tenability and high

photostability (Walling et al. 2009). However, organic fluorophores are prone to photobleaching and there is the problem of synthesis, storage and toxicity with heavy metal-based semiconductor fluorophores. Thus, we need a fluorophore which overcomes problems described above while combining the advantages they offer. Carbon quantum dots present an attractive option in this regard and are gaining increasing application in biosensing and bioimaging because they display excellent stable photoluminescence, high resistance to photobleaching and low toxicity (Lim et al. 2015; Li et al. 2012; Shi et al. 2014). Moreover, their synthesis is relatively simple, inexpensive and non-toxic (Peng and Travas-Sejdic 2009; Derfus et al. 2004; Chunduri et al. 2016). Along with excellent water solubility and good biocompatibility, these properties make carbon dots sensitive and cost-effective candidates for fluorescent biolabels (Ding et al. 2014; Zuo et al. 2015; Hu 2013).

Thus, integrating the simplicity of a paper-based immunoassay platform with highly versatile photoluminescent carbon dots, we have designed a carbon dot-based immunoassay protocol on a paper substrate. HIV-1 p24 was chosen as the antigen for implementing this assay for early detection of HIV-1 p24 for the reasons mentioned above. The results presented in this study can pave the way for CDPIA to be effectively used for rapid screening of early HIV infection and to provide medical care expeditiously and therefore control and prevent the spread of this disease.

2 Materials and methods

2.1 Chemicals and reagents

The following were used in our study: Whatman filter paper Grade 1, nitrocellulose membrane, wax pencils, anhydrous citric acid (Sigma), Triton X-100 (Sigma), sodium borohydride (Himedia), glutaraldehyde (Himedia), ethylene diamine (Himedia), streptavidin (Scripps Lab, USA), casein block buffer (Thermo Scientific, USA), anti-HIV-1 p24 antibody (Prospec, USA), HIV-1 p24 antigen (Virogen, USA), biotinylated HIV-1 p24 detector antibody (PerkinElmer, USA). Phosphate buffer saline (100 mM, pH-7.2) and carbonate bicarbonate buffer (500 mM, pH-9.5) were prepared by reported procedures. Centrifugal spin columns (10, 30, 100 kDa) were purchased from GE Health Care, UK. All experiments were performed with double-distilled water.

Plasma samples from patients and healthy individuals were obtained from the Sri Sathya Sai Institute of Higher Medical Sciences, Prasanthigram, India (Study Id—SSIHL/IEC/PSN/BS/2012/01). The samples were coded and tested in blinded manner with fourth-generation Microlisa HIV Ag+Ab ELISA kit (J. Mitra & Co. Pvt. Ltd.).

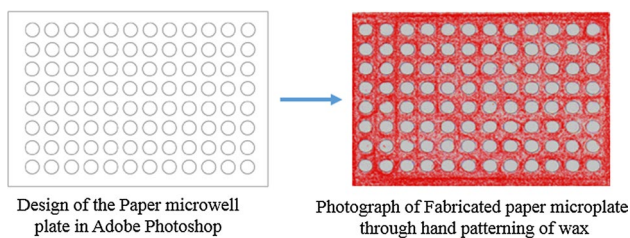


Fig. 1 Designing of the 96-well paper microwell plate. The *red color* on the paper indicates the wax patterned area (color figure online)

2.2 Designing of the paper microplate

The paper microplate was designed in the software Adobe Photoshop 5 based on the design of a standard 96-well microplate. The paper microwell plate design consisted of 8 rows of 12 wells each of 6 mm diameter spaced 2 mm apart. The dimension of the plate was 105 mm × 70 mm. The design was transferred onto the Whatman filter paper and nitrocellulose paper using a printer.

2.3 Device fabrication

As illustrated in Fig. 1, the Whatman filter paper was covered with wax to create the hydrophobic boundaries for the 96 wells. The paper was heated at 185 °C for 90 s on the hot plate (Ma et al. 2014). The hydrophobic wax melted and penetrated through the porous paper, and well-defined hydrophilic wells were created. Similarly, nitrocellulose paper was also wax patterned at 125 °C for 45 s (Lu et al. 2010). The wells were tested for their hydrophilic nature by wetting with water.

2.4 Synthesis of carbon dots

Carbon dots were synthesized using a simple one-step hydrothermal technique (Wu et al. 2015; Zhu et al. 2013). 0.84 g of citric acid and 1.06 mL of ethylene diamine were dissolved in 20 mL of ultrapure water in the molar ratio of 1:4. The solution was then transferred to a 100 mL Teflon hydrothermal reactor and heated in an oven for 5 h at 180 °C. Subsequently, the reactor was removed and allowed to cool to room temperature. The resulting C-Dot solution was lyophilized and stored for characterization and immunoassay experiments.

2.5 Characterization of the carbon dots

The topography, morphology and size of the carbon dot dispersion were characterized using a JEOL, 2100F Transmission Electron Microscope operated at 200 kV. The carbon

dots were drop casted on the copper grid and vacuum-dried before imaging.

Shimadzu 2450 UV–Vis spectrophotometer and SpectraMax M5 microplate reader were used to perform the optical characterization and measurements. The samples were diluted accordingly before being used to obtain absorbance and fluorescence spectra. FTIR spectra were obtained using potassium bromide (KBr) pellet method on Thermo Scientific Nicolet *is10* FTIR spectrometer.

2.6 Bioconjugation of carbon dots with streptavidin

A glutaraldehyde-mediated conjugation procedure was carried out to bioconjugate the above purified carbon dot solution (Wu et al. 2015). To 4.5 mL (173 mg/mL) of carbon dots, 900 μL of Sodium bicarbonate buffer (500 mM, pH 9.5) was added. To this mixture, 300 μL of 5 % (w/v) glutaraldehyde solution was added dropwise with stirring. The above mixture was left for stirring for 1 h at room temperature.

Thereafter 300 μL of 2.7 mg/mL of streptavidin in phosphate buffer saline (PBS) solution was introduced dropwise with stirring into the reaction mixture, and the reaction was allowed for 1 h and then transferred to an ice bath. Subsequently, 1.2 mL of freshly prepared sodium borohydride (20 mg/mL) was added dropwise to the reaction mixture in the ice bath and incubated overnight at 4 °C. The streptavidin-conjugated carbon dots were filtered through centrifugal spin columns (10 and 30 kDa MWCO) and washed several times with PBS buffer.

2.7 Fluorescence polarization

In order to verify the conjugation of carbon dots with streptavidin, fluorescence polarization studies were carried out wherein the fluorescence polarization value for conjugated and unconjugated carbon dots was compared. The excitation and emission wavelengths were chosen as 348 and 453 nm, respectively. The fluorescence polarization value was calculated from the formula (Lea and Simeonov 2011).

$$FP = \frac{I_{\parallel} - G \times I_{\perp}}{I_{\parallel} + G \times I_{\perp}} \quad (1)$$

where FP is Fluorescence polarization. I_{\parallel} is the parallel polarized emission, I_{\perp} is the perpendicularly polarized emission and G is the correction factor which is evaluated for the sensitivity of the instrument.

The I_{\parallel} and I_{\perp} were measured in the fluorescence polarization mode by SpectraMax M5 and substituted in the above formula to obtain the FP ratio. The higher magnitude of FP for the post-conjugation step compared with

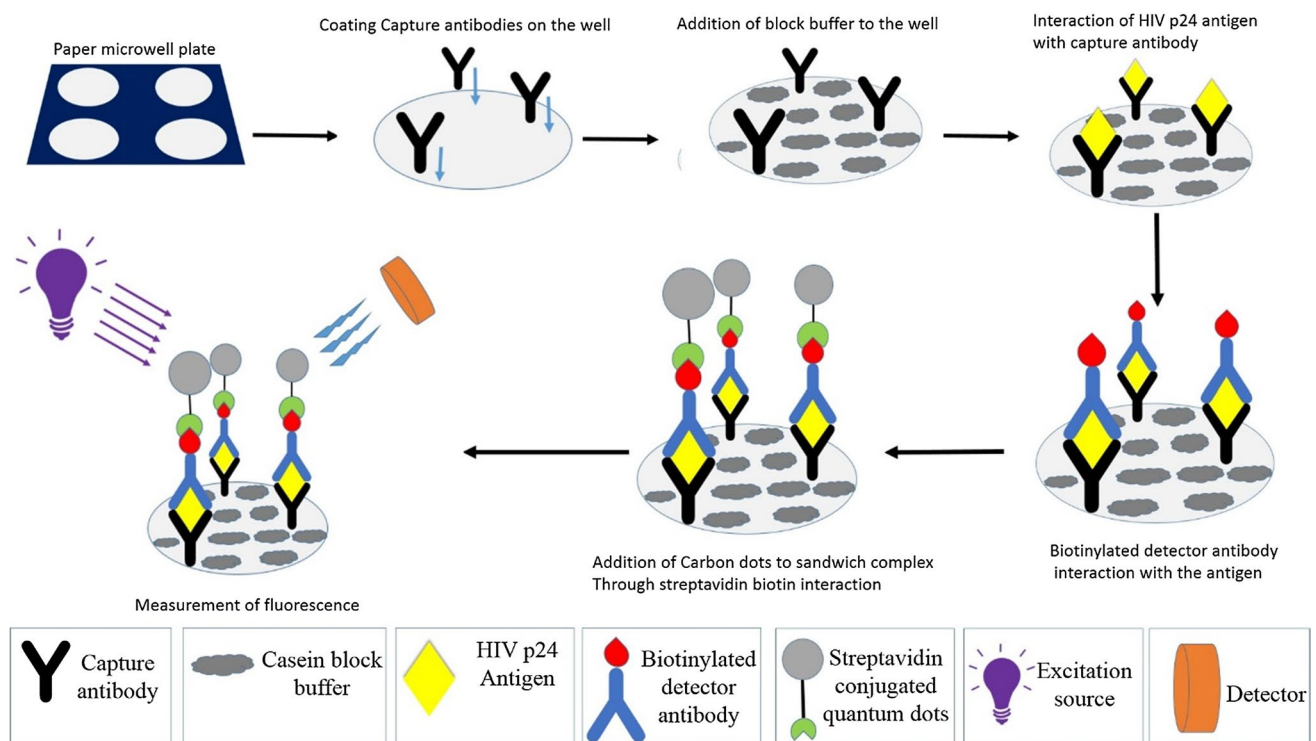


Fig. 2 Schematic of steps involved in CDPIA

unconjugated carbon dots confirmed conjugation of carbon dots to streptavidin.

2.8 Carbon dot-based paper immunoassay (CDPIA) for detection of HIV-1 p24 antigen

2.8.1 Whatman filter paper

The steps involved in CDPIA on Whatman filter paper (CDWIA) are depicted in Fig. 2. Primary (capture) antibody was immobilized on the test zone of paper microplate through the process of physical adsorption by adding 5 μL of antibody solution onto the wells. After 10 min, 5 μL of casein block buffer solution (50 mg/mL) was added to each test zone to prevent non-specific binding of the antigen to the detection region. Upon drying, antigen concentrations ranging from 10 to 250 $\mu\text{g}/\text{mL}$ were added to the wells. The paper microwell plate was left for incubation for 15 min after which it was dried under a stream of ambient air. The dried paper microplate was then immersed in wash buffer (PBS solution containing 0.5 % Tween-20) for 45 s and then dried again to remove the non-specifically adsorbed antigen from the paper. Subsequently, biotinylated secondary (detector) antibody solution was dropped onto each well and allowed to incubate for 15 min. After a round of washing and drying step to remove non-specifically

absorbed detector antibody, 5 μL of streptavidin-conjugated carbon dots was added to each well and incubated for 15 min. This step was followed with a final round of washing and drying. The dried paper microwell plate was then placed in the SpectraMax M-5 microplate reader, and the signal intensities were measured for each well. The CDWIA was performed on each concentration of antigen in triplicate.

2.8.2 Nitrocellulose paper

The same procedure used for CDWIA was followed for CDPIA on nitrocellulose paper (CDNIA) with varying antigen concentration except the incubation period which was shortened to 5 min.

2.8.3 Control experiment

In order to study the effect of any interference for other proteins, a control experiment was performed with bovine serum albumin as the interfering protein. Five concentrations of BSA were taken in the range of 10 $\mu\text{g}/\text{mL}$ –100 ng/mL , and its effect on the fluorescence intensity was noted at the p24 antigen concentration of 1 ng/mL . With the above parameters, CDNIA was performed on the samples in triplicate and the effect of the interfering protein was studied.

2.9 HIV detection in blood plasma samples

2.9.1 Preparing plasma samples

Blood samples obtained were initially confirmed to be HIV negative using standard HIV detection ELISA test kits (third and fourth generation ELISA kits). 2 μ L of plasma was diluted in 188 μ L casein block buffer, and 10 μ L of 10 % aqueous solution of Triton X-100 was added to prepare the test sample.

2.9.2 HIV-1 p24 spiked plasma samples

To check the efficacy of our detection system, HIV-1 p24-negative plasma samples spiked with known concentrations of p24 antigen were tested. This solution was serially diluted with PBS solution to obtain desired concentrations. The samples were then subjected to CDNIA and the per cent recovery was calculated by the formula

$$\text{Recovery \%} = \frac{\text{Measured concentration}}{\text{Actual concentration}} \times 100$$

To establish the clinical validity of our paper-based immunoassay, CDNIA was evaluated using 10 HIV-positive and 15 HIV-negative clinical samples.

2.10 Testing the specificity of CDPIA protocol

To evaluate the specificity of the protocol, plasma containing hepatitis C virus was spiked with p24 antigen and the effect on the fluorescence intensity was observed. The plasma containing HCV was serially diluted 5-, 10-, 20-, 50- and 100-fold and was spiked with p24 antigen to obtain the fixed concentration of 1 ng/mL in the final sample solution. The CDNIA protocol was applied to the thus prepared sample, and the fluorescence intensities were noted.

3 Results and discussion

3.1 Design and fabrication of paper microwell plate

The 96-well plate design is a standard and an efficient template for multiplexing which makes it an excellent choice as a template for our paper microplate. Moreover, the microplate reader has compatibility with the 96-well plate design, thus ensuring proper detection.

The novel method of hand patterning of wax on paper is both convenient and feasible because of the simplicity of the technique and more importantly, the process and materials used are inexpensive. One of the challenges is to ensure that the wax has completely penetrated the pores of the paper to establish the hydrophobic barrier. Time and

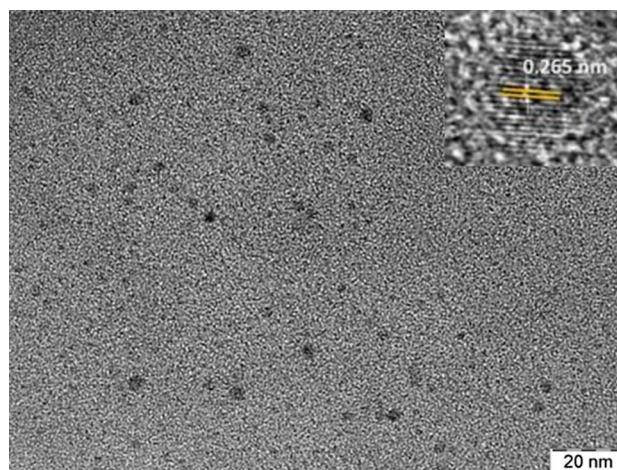


Fig. 3 TEM image of carbon dots which indicates the size of the carbon dots to be around 5 nm. The *inset* shows the HRTEM image of carbon dots with the interplanar spacing

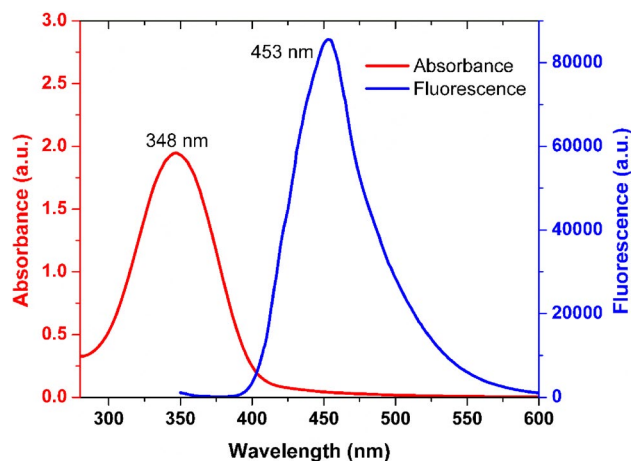


Fig. 4 UV-Vis absorbance and fluorescence emission spectra of carbon dots

temperature are crucial parameters to optimize diffusion of wax through the pores without surface diffusion onto the test zones. The optimal temperature and time conditions of heating the paper microplate to 185 $^{\circ}$ C for 90 s for the Whatman filter paper and 125 $^{\circ}$ C for 45 s for the nitrocellulose filter paper gave very well-defined hydrophobic barriers that, when tested by wetting with water, gave proper circular hydrophilic test zones.

Another factor which affects the hydrophobic barriers at a given temperature is the thickness of the wax coat. While insufficient wax can cause an irregular hydrophilic barrier, thus allowing solvents to leak into the coated region, excess of wax can lead to excess internal diffusion making the test zones hydrophobic and rendering them unsuitable for use. Thus, the optimum amount of wax was coated by applying

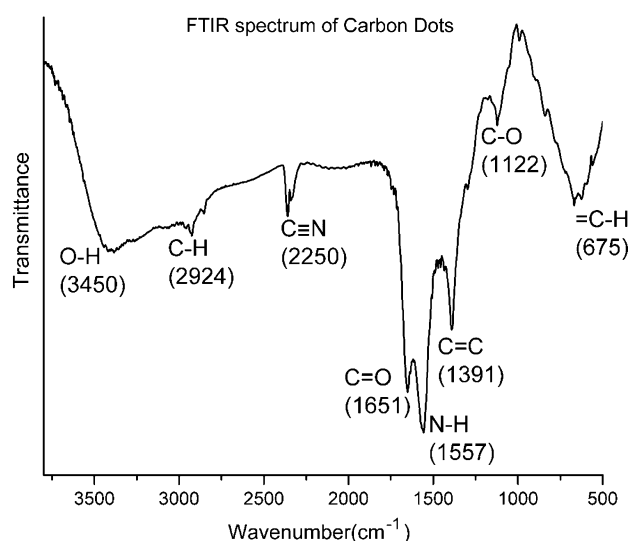


Fig. 5 FTIR spectrum of carbon dots

two coats of wax using a wax pencil. A dark-coloured wax pencil can ascertain sufficient contrast with the white paper which can help to visibly distinguish the coated hydrophobic part from the uncoated hydrophilic zones.

3.2 Characterization of carbon dots

TEM was able to confirm the size and morphology of the carbon dots. From the TEM images, the size of the carbon dots was confirmed to be 4–5 nm and of mostly spherical morphology (Fig. 3). The HRTEM showed the interplanar spacing to be 0.265 nm which is the standard reported value in the literature (Wu et al. 2015).

The optical properties of the carbon dots were studied using UV–Vis spectroscopy and photoluminescence studies. As illustrated in Fig. 4, the absorption spectra revealed a broad peak in the range of 300–400 nm, which can be attributed to typical $n-p^*$ transition of the carbonyl group (Hsu and Chang 2012; Zhu et al. 2012). A brilliant blue fluorescence emission is observed when the carbon dot solution is subjected to UV light (365 nm) which is visible to naked eyes. A broad emission centred at 453 nm was observed in the emission spectrum with an excitation wavelength peak at 348 nm.

Meanwhile, the FTIR studies were carried out to understand the surface functional groups present on the carbon dots (Fig. 5). The presence of the carboxylic group was confirmed by characteristic absorption bands of O–H (3450 cm^{-1}), the stretching vibration band of C=O (1651 cm^{-1}) and the stretching vibration bands of C–O (1122 cm^{-1}) (Zhu et al. 2012). Furthermore, one sharp peak at 1557 cm^{-1} assigned to the vibration and deformation bands of N–H, and a small peak at 2250 cm^{-1} assumed to be $\text{C}\equiv\text{N}$ indicates the existence of amino-containing

Table 1 Comparison of fluorescence polarization value of the unconjugated carbon dots with the conjugated carbon dots

Sample	I_{\parallel}	I_{\perp}	$FP = \frac{I_{\parallel} - G \times I_{\perp}}{I_{\parallel} + G \times I_{\perp}}$
Unconjugated Carbon dots	114.82	102.54	0.056
Streptavidin-conjugated carbon dots	184.48	156.95	0.081

I_{\parallel} is the parallel polarized emission, I_{\perp} is the perpendicularly polarized emission, and FP is the fluorescence polarization value

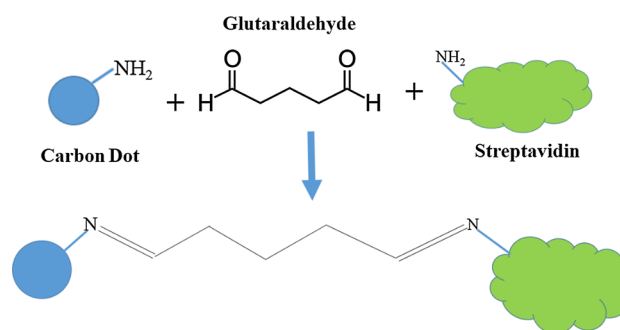


Fig. 6 Schematic of conjugation of carbon dots to streptavidin through glutaraldehyde

functional groups which is necessary for streptavidin conjugation (Hsu and Chang 2012; Liang et al. 2013). Moreover, the three obvious absorption peaks at 2924, 1391 and 675 cm^{-1} are associated with the stretching and bending vibrations of C–H, C=C and $=\text{C}-\text{H}$, respectively, suggesting the presence of alkyl and aryl groups (Roy et al. 2015).

3.3 Fluorescence polarization studies

The fluorescence polarization studies were conducted on the SpectraMax M5 plate reader in the fluorescence polarization mode. The correction factor (G) of the plate reader was calculated to be 1. The results are depicted in Table 1.

The conjugation of carbon dots is confirmed by the higher value of its fluorescence polarization value (0.081) compared to the unconjugated carbon dots (0.056). This is explained by the correlation between fluorescence polarization and size of the fluorophores. The smaller size of the unconjugated particle causes their movement in solution which leads to depolarization of the incident plane polarized excitation energy, thus leading to very low polarization value (Lea and Simeonov 2011; Fluorescence Polarization 2010). However, in case of conjugation of carbon dots to streptavidin, the motion of the particle is reduced due to an increase in the size and volume of the particles (Fig. 6). As the rotation of particle reduces, the excitation energy and the transmitted energy are nearly in the same state of polarization which is expressed as a higher magnitude of

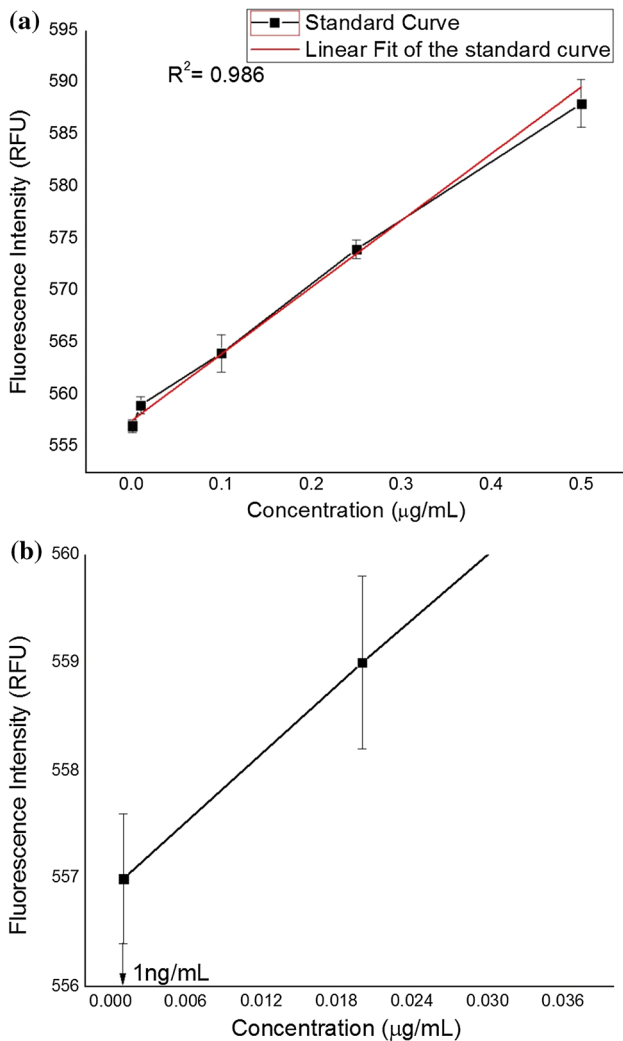


Fig. 7 **a** Plot of standard curve for CDWIA. The red line indicates the fitting curve obtained by linear regression. **b** Standard plot of CDWIA with resolved axis that points to the lower detection limit of CDWIA (color figure online)

polarization value (Bruno et al. 2005). Thus, the polarization value for the conjugated particle is higher than that of the unconjugated particle.

3.4 Results of CDPIA

3.4.1 Whatman filter paper

The results of the CDWIA with carbon dots as the fluorescent label are depicted in Fig. 7a, b. The assay exhibited linear correlation when tested in the range of 10 µg/mL–1 ng/mL as evident from the standard plot and the lower detection limit of HIV-1 p24 was found to be 1 ng/mL. Since the volumes used were 5 µL, this directly translates to a

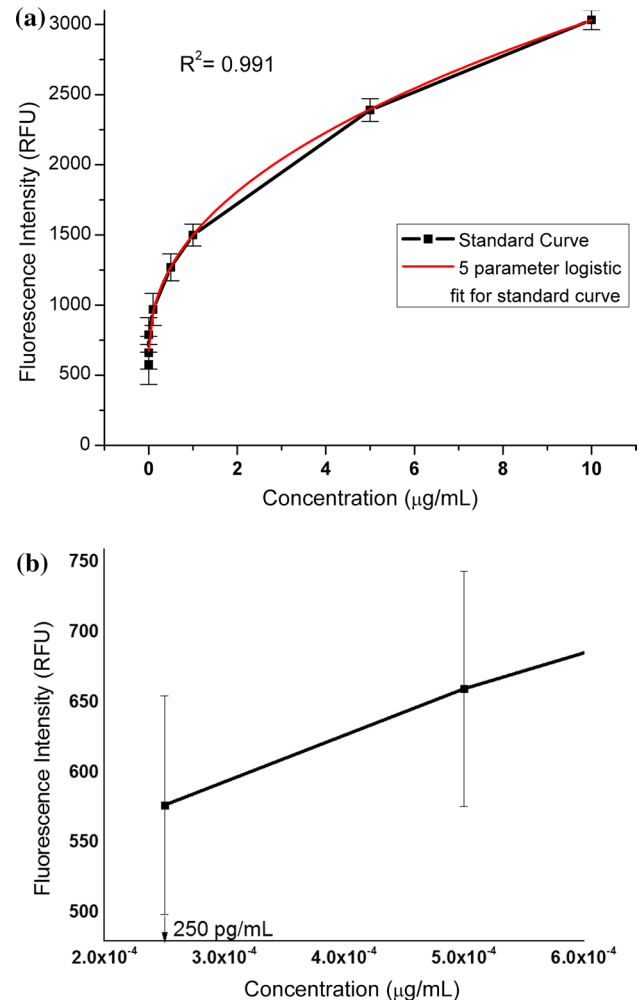


Fig. 8 **a** Plot of standard curve for CDNIA. The red line indicates the fitting curve obtained by five-parameter logistic regression. **b** Plot of standard curve of CDNIA with resolved axis that points to the lower limit of detection of CDNIA (color figure online)

detection of 5 pg of HIV-1 p24 per well. The linear coefficient of correlation was found out to be 0.986, indicating it to be a linear dose-dependant model. The fluorescence signals observed for concentrations till 1 ng/mL were clearly higher than the signal observed for a blank well. But for concentrations below 1 ng/mL, the signal could not be clearly attributed to the presence of antigen and could be a result of non-specific absorption of the carbon dots on paper. This arises out of the porous nature of cellulose which leads to the non-specific absorption of antigens, antibodies and carbon dots by hydrophobic and electrostatic interaction (ROWLAND 1977).

Whatman filter paper offers a large surface area with high absorptivity which simplifies the process of immobilization of antibodies on the well by the process of physical adsorption (Kim and Herr 2013). This results

in drastic reduction in the duration required for coating antibodies onto the detection zone. The addition of sample solution containing the HIV-1 p24 antigen followed by addition of detector antibody results in the formation of a sandwich which is crucial for the detection. The interaction between biotinylated detector antibody, which is part of the sandwich, and the streptavidin-conjugated carbon dots added to the wells can be attributed to the strong non-covalent interaction between streptavidin and biotin molecules (Tang and Hewlett 2010). This interaction is crucial to detection as exposure to excitation signal would cause the carbon dots to fluoresce and indicate the presence of the antigen.

3.4.2 Nitrocellulose paper

The advantage of using nitrocellulose paper is that it has a very high absorption capacity for proteins compared to Whatman filter paper (Fenton et al. 2009). There is a two-fold interaction which strengthens the immobilization of the capture antibodies on the well. Firstly, a dipolar interaction forms between the nitro groups of the paper and the carbonyl groups of the antibody. Additionally, the hydrophobic part of nitrocellulose interacts with the hydrophobic domains of the protein (Desiderio 1990). These interactions cause large amounts of capture antibodies to be absorbed onto the paper in a shorter period, thus reducing the incubation period. This strong absorption leads to a large amount of capture antibodies being coated on the well, and they remain immobilized during the wash step. As a result, the efficiency of the immunoassay is higher on nitrocellulose membrane compared to the Whatman filter paper.

Even in terms of sensitivity, nitrocellulose paper scores above Whatman filter paper as seen in the standard curve plotted in Fig. 8a, b. The nitrocellulose paper showed good sensitivity with a lower detection limit of 250 pg/mL which indicates detection of 1.25 pg of HIV-1 p24 per detection zone. It was also noted that the incubation period for the assay was reduced to 5 min. The results showed that CDNIA was fourfold more sensitive than CDWIA and reduced the assay duration by threefold. It was observed that the data fitted well to five-parameter logistic model (which is a superior model for fitting in immunoassays) which established the correlation between the p24 concentrations and corresponding fluorescence intensities. The coefficient of correlation (R^2) was calculated to be 0.991.

While the nitrocellulose paper did show good sensitivity in HIV-1 p24 detection compared to Whatman filter paper, the sensitivity of CDNIA can be improved further by the choice of better papers which are specifically designed with reduced autofluorescence, thus improving the limit of detection to femtogram-level concentrations.

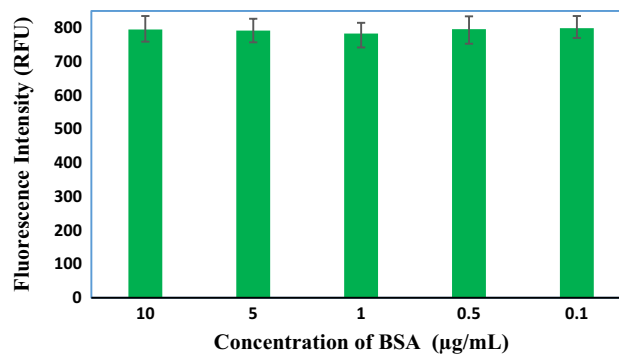


Fig. 9 Effect of the presence of BSA as an interfering protein on CDNIA protocol

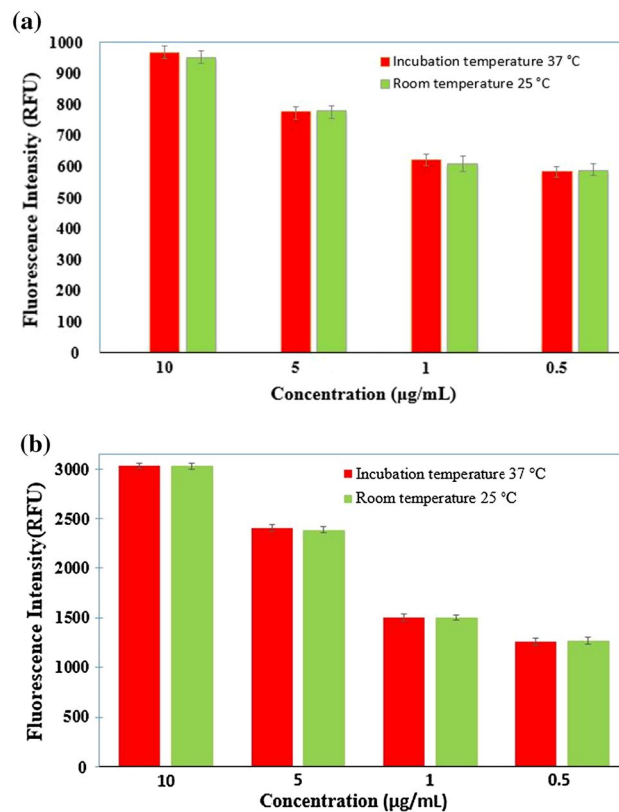


Fig. 10 a Effect of incubation temperature on the CDWIA. b Effect of incubation temperature on the CDNIA

3.4.3 Control experiment effect of BSA as an interfering protein

It was observed that the presence of bovine serum albumin had hardly any effect on the fluorescence intensities for a fixed concentration of p24. As evident from Fig. 9, increasing the concentration of BSA had negligible effect on the fluorescence measurements. This goes on to reiterate the stability and specificity of the protocol.

3.4.4 Effect of temperature on the immunoassay

The effect of incubation temperature was studied using both Whatman filter paper and nitrocellulose paper by comparing the results of the immunoassay performed at incubation temperature of 37 °C with the immunoassay performed at room temperature of 25 °C (Fig. 10). The results showed negligible difference in the signal intensities which clearly indicates that the paper microplate can be incubated at room temperature. A possible reason for this could be as follows. The collision theory of reactions assumes that the frequency of the interaction of the reactants, in this case the antibody and antigen, determines the rate of reaction. The incubation temperature provides energy to the reactants so that a sufficient number of vigorous interactions occur to form the antigen–antibody complex. In case of paper as the substrate, the number of interactions is already high due to a smaller detection zone, high surface-to-volume ratio and porosity of the paper. This allows more interactions to occur compared to a microwell plate. As a result, room temperature is a sufficient enough temperature condition for incubation (Zang et al. 2012). Thus, the present CDPIA like other paper-based assays also does not require specialized equipment for incubation (Mu et al. 2014; Ge et al. 2012).

3.4.5 Optimization of the capture antibody concentration

The concentration of capture antibodies is an important factor in the sensitivity of the immunoassay. There is an optimal concentration of capture antibody at which the signal will be highest; at higher concentrations, the background signal is also higher and concentrations below this the signal will be weaker (Liu et al. 2014). Optimization of concentration of capture antibody required for the assay was done by testing different concentrations of 10, 20, 50 $\mu\text{g}/\text{mL}$. As shown in Fig. 11a, b, for 10 and 20 $\mu\text{g}/\text{mL}$ the signal response was poor and there was no good correlation between the observed signal and antibody concentration. However, at 50 $\mu\text{g}/\text{mL}$, there was a strong response observed with both papers. For concentrations higher than 50 $\mu\text{g}/\text{mL}$, there was no change in the response which can be attributed to the saturation of the detection area with capture antibodies at 50 $\mu\text{g}/\text{mL}$. As a result, 50 $\mu\text{g}/\text{mL}$ was chosen as the optimal concentration of capture antibody for further experimentation.

3.4.6 Optimization of Carbon dots concentration

Carbon dots being the reporting labels, their concentration greatly affects the efficiency of the assay. The assay was performed with five different concentrations of

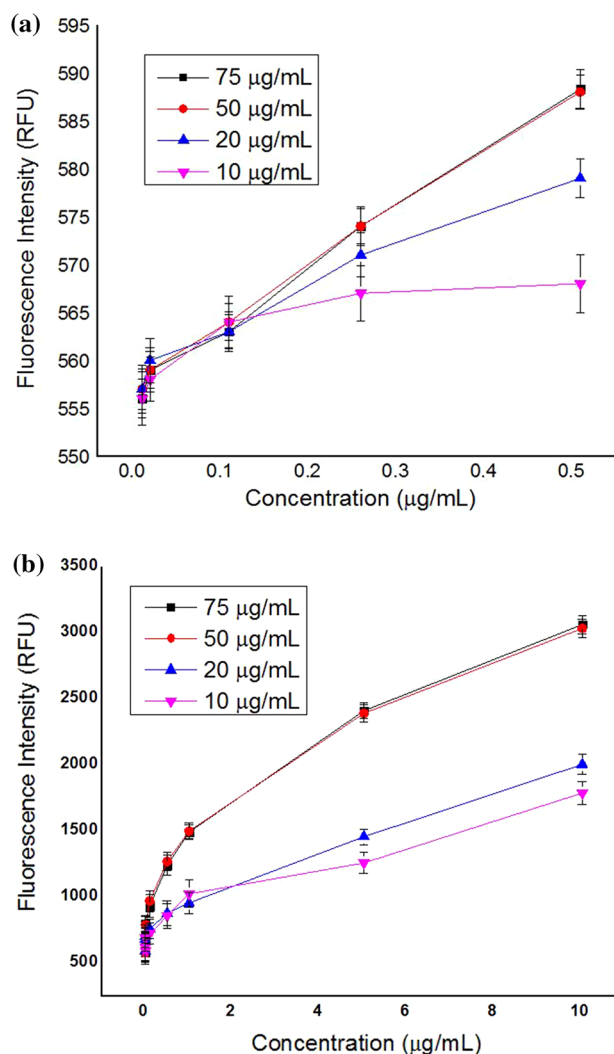


Fig. 11 a Effect of capture antibody concentration on CDWIA. b Effect of capture antibody concentration on CDNIA

carbon dots, 20, 50, 100, 150 and 200 $\mu\text{g}/\text{mL}$ for a fixed concentration of capture antibody of 50 $\mu\text{g}/\text{mL}$ and antigen concentration of 1 $\mu\text{g}/\text{mL}$. The signal from blank wells (without antigen) was also measured for the different concentrations of carbon dots and the signal-to-blank ratio was calculated and plotted. As seen from Fig. 12a, b, the signal-to-blank ratio increased with the increase in the concentration of carbon dots till 100 $\mu\text{g}/\text{mL}$ for Whatman filter paper and 150 $\mu\text{g}/\text{mL}$ for nitrocellulose paper after which there was decrease in the ratio owing to the increase in the intensity of blank. This can be attributed to the increased non-specific absorption of carbon dots on the paper with an increase in the concentration of the carbon dots. Thus, the optimal concentration of carbon dots is 100 $\mu\text{g}/\text{mL}$ for Whatman filter paper and 150 $\mu\text{g}/\text{mL}$ for nitrocellulose paper.

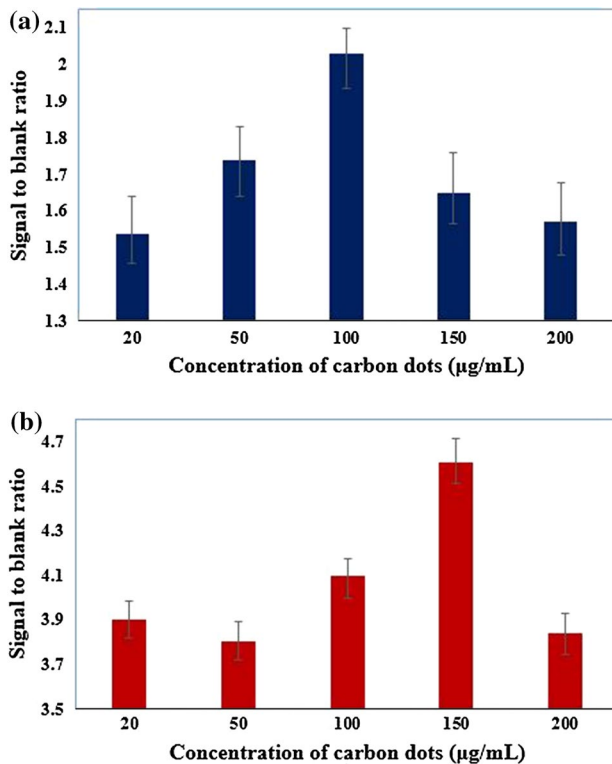


Fig. 12 a Effect of carbon dots concentration on CDWIA. b Effect of carbon dots concentration on CDNIA

Table 2 Recovery percentage for HIV-1 p24 antigen spiked in the HIV-negative plasma samples

Sample	Spiked concentration	Measured concentration	Recovery (%)
1	10 µg/mL	9.5 ± 0.4 µg/mL	95.0 ± 4
2	5 µg/mL	4.70 ± 0.3 µg/mL	94.0 ± 6
3	2.5 µg/mL	2.40 ± 0.17 µg/mL	96.0 ± 6.8
4	1 µg/mL	1.01 ± 0.04 µg/mL	101.0 ± 4
5	500 ng/mL	477.0 ± 28.0 ng/mL	95.4 ± 5.6
6	100 ng/mL	98.6 ± 3.6 ng/mL	98.6 ± 3.6
7	500 pg/mL	491.6 ± 9.0 pg/mL	98.3 ± 2
8	250 pg/mL	251.2 ± 8.3 pg/mL	100.4 ± 3.3

3.5 HIV detection in blood plasma samples

The spiked plasma samples that were tested using the protocol showed excellent per cent recovery in the range from 94 to 101 %. This implies that the assay can detect HIV-1 p24 close to its actual concentration even in the plasma samples. Thus, the efficiency of CDPIA with the clinical plasma samples is as good as with test samples. The per cent recovery is tabulated in Table 2.

To evaluate the clinical specificity of the assay in clinical samples, we tested 15 plasma samples from confirmed HIV-negative individuals and 10 plasma samples from confirmed HIV-positive individuals. The CDPIA showed no false positives when HIV-negative samples were tested. The fluorescence signal from these samples was comparable or lower than the blank signal intensity. It may be observed that the varying fluorescence intensities of the positive samples indicate the different stages of disease progression in the body. The increasing intensity directly correlates with the increasing amount of p24 in the plasma which points at the progression of the disease in the patient. Ten HIV-positive samples on which CDPIA was performed tested positive (Fig. 13a), whereas 15 HIV-negative samples were tested by CDPIA and were confirmed as negative (Fig. 13b). With 100 % accuracy, CDPIA has the potential to be a point-of-care tool for rapid detection of HIV.

3.6 Evaluation of specificity of CDPIA

The specificity of CDPIA protocol was tested with hepatitis C virus as the competing moiety. The results of the CDNIA performed on p24 concentration of 1 ng/mL are depicted in Fig. 14. It is quite clear that there is no effect of the varying concentration of HCV on the fluorescence intensities of p24 detection.

3.7 Comparison between CDPIA and conventional ELISA

As stated before, the main advantage of our CDPIA is that it is relatively rapid and consumes minimal amount of reagents and hence cost-effective compared with conventional immunoassay techniques. The sensitivity of CDPIA is lower compared to the conventional ELISA which can detect up to 10–20 pg/mL of target analyte (Tang and Hewlett 2010). This was due to the autofluorescence of the paper which prevented detection of lower concentrations of p24.

A comparison of the experimental parameters between the CDPIA and ELISA is given in Table 3. As depicted in table, CDPIA consumes <10 % of reagents used in conventional ELISA and can be carried out in <30 min.

To gain an insight into the efficiency of the CDPIA, we need to have a closer look at the device itself. The thin hydrophobic wax barrier greatly influences the process as it provides higher surface area for the interaction while reducing the device dimension and facilitating for smaller sample volume for processing (Jeong et al. 2015). The highly porous cellulose allows uniform spreading of the applied reagent by wicking process which wets the detection area completely and transports the reagent throughout the bulk of the detection area (Tenda et al. 2016). Now cellulose is a

Fig. 13 **a** CDNIA applied to 10 HIV-positive samples and compared with the results from blank and a HIV-negative sample. The blue black and red bars denote the positive blank and the highest measured negative samples, respectively. **b** CDNIA applied to 15 HIV-negative samples which are compared with the result from a blank and a HIV-positive sample. The red, black and blue bars denote the negative, blank and the lowest measured positive samples, respectively

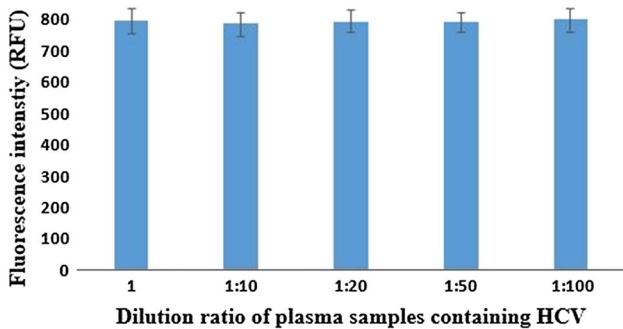
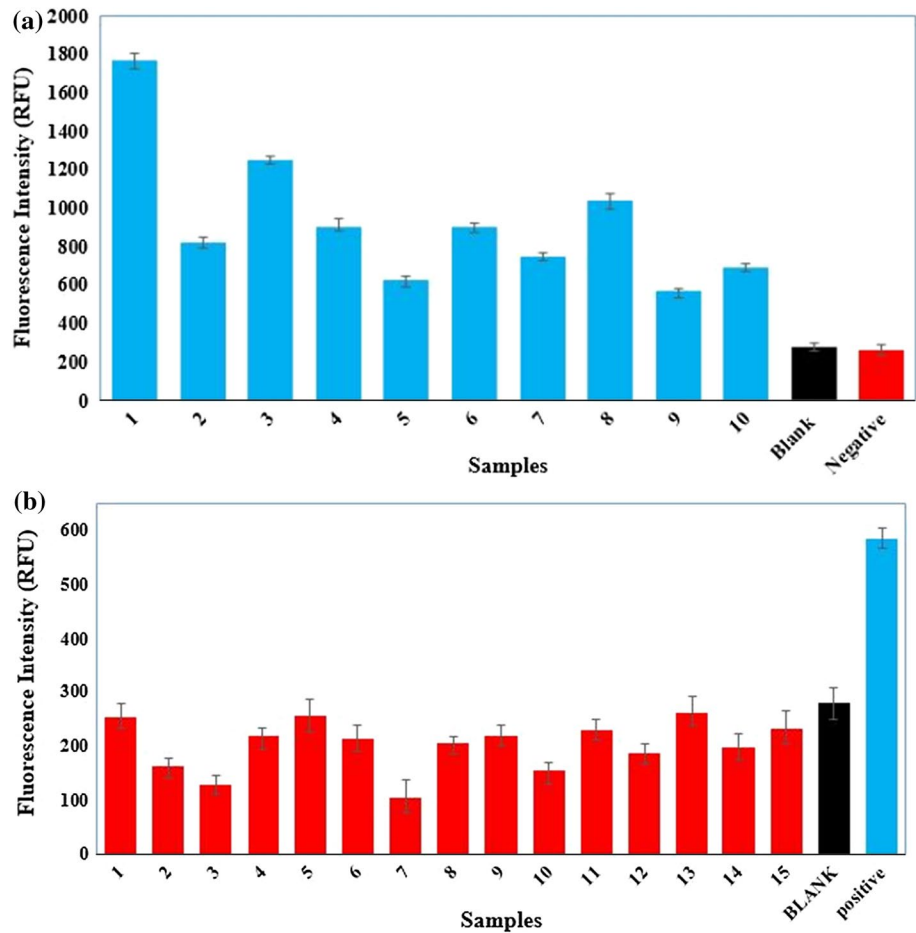


Fig. 14 Effect of varying dilution of HCV on the fluorescence intensities from CDNIA performed on p24 sample

polysaccharide made of polymeric chains of D-glucose molecules which is hydrophilic due to the presence of large number of -OH groups. These hydroxyl functional groups in turn allow binding of antibody to the cellulose fibres (Heiat et al. 2014). A large number of antibodies can be bound to the nitrocellulose which has high surface area due to its porosity. When the sample is introduced, this large surface area also allows higher number of interactions between the antigen

and the antibody (Samyn 2013). As a result, even though the sample volume is less, the higher number of interactions can produce a readable signal intensity (Zhao and van den Berg 2008). Thus, a small volume droplet should be sufficient for the immunoassay to be performed. Table 4 gives a few examples where the small sample volumes have been applied for successful and sensitive detection of target analytes on paper.

4 Conclusions

A highly efficient and rapid paper-based sandwich immunoassay on Whatman filter paper and nitrocellulose paper were developed for the detection of HIV-1 p24 antigen using carbon dots as the fluorescent reporter. The carbon dots were synthesized from citric acid and ethylene diamine and conjugated with streptavidin using glutaraldehyde. Paper was patterned using a hand-printing technique. The detection range was 10 µg/mL to 1 ng/mL for the Whatman filter paper while the nitrocellulose paper exhibited a higher range from 10 µg/mL to 250 pg/mL. CDPIA on the nitrocellulose paper (CDNIA) exhibited four times higher sensitivity and reduced the assay time by three times compared

Table 3 Comparison of volumes of reagent and time periods for various steps in CDPIA and conventional immunoassay

Reagents	CDPIA				Conventional ELISA	
	Whatman paper		Nitrocellulose paper		Volume (μL)	Time (min)
	Volume (μL)	Time (min)	Volume (μL)	Time (min)		
Capture ab immobilization	5	10	5	5	100	1440
Blocking buffer	5	15	5	5	100	30
HIV-1 p24 antigen	5	15	5	5	100	60
Detector ab immobilization	5	15	5	5	100	60
Detection step	5	15	5	5	100	30

Table 4 Comparison of detection of lowest concentration

S no	Target analyte	Sample volume (μL)	Concentration detected	References
1	DNase	1	Few nM	Zhao et al. (2008)
2	BSA	1	0.38 μM	Martinez et al. (2007)
3	Tumour marker CEA	3	5 ng/mL	Ge et al. (2012)
4	E Coli.	5	57 CFU/mL	Ma et al. (2014)
5	Rabbit IgG	5	67 pmol	Cheng et al. (2010)
6	HIV-1 p24	5	250 pg/mL	Present work

to CDPIA on Whatman paper (CDWIA). HIV-negative and HIV-positive plasma samples were tested using CDPIA for the detection of HIV-1 p24. Both immunoassays exhibited no false-positive and false-negative results when used to test a limited number of clinical samples and also indicated near 100 % recovery rates. Thus, the CDWIA and CDPIA systems we developed have demonstrated that carbon dots may be excellent biolabel reporters for diagnostic tests. Further, the one-step synthesis procedure and high photostability of the carbon dots can potentially result in consistent and reproducible performance of the assay.

Acknowledgments All authors are grateful to Bhagawan Sri Sathya Sai Baba for his constant inspiration and guidance. Aditya Kurdekar thanks DST for their support through the DST-INSPIRE Fellowship program, Ministry of Science and Technology, Government of India. L. A. Avinash Chunduri acknowledges UGC, Government of India for BSR fellowship. We acknowledge with gratitude Prof. S. Sampath for providing the TEM facility for characterization.

References

- AIDS GLOBAL STATISTICS (2015) www.aids.gov
- Anderson RM et al (1986) A preliminary study of the transmission dynamics of the human immunodeficiency virus (HIV), the causative agent of AIDS. *IMA J Math Appl Med Biol* 3(4):229–263
- Bartlett PA, Entzeroth M (eds) (2006) Exploiting chemical diversity for drug discovery. Royal Society of Chemistry, Cambridge. doi:10.1039/9781847552556. <http://ebook.rsc.org/>
- Bruno A, de Lisio C, Patrizia M (2005) Time resolved fluorescence polarization anisotropy of carbonaceous particles produced in combustion systems. *Opt Express* 13(14): 5393–5408. <https://www.osapublishing.org/oe/abstract.cfm?uri=oe-13-14-5393>
- Cheng C-M et al (2010) Paper-based ELISA. *Angew Chem Int Ed Engl* 49(28):4771–74. <http://www.ncbi.nlm.nih.gov/pubmed/20512830>
- Chunduri LA et al (2016) Carbon quantum dots from coconut husk: evaluation for antioxidant and cytotoxic activity. *Mater Focus* 5(1): 55–61. <http://openurl.ingenta.com/content/xref?genre=article&issn=2169-429X&volume=5&issue=1&page=55>
- Derfus AM, Chan WC, Bhatia SN (2004) Probing the cytotoxicity of semiconductor quantum dots. *Nano Lett* 4(1):11–18. doi:10.1021/nl0347334
- Desiderio DM (1990) Mass spectrometry of peptides. CRC Press, Boca Raton. <https://www.crcpress.com/Mass-Spectrometry-of-Peptides/Desiderio/9780849362934>
- Ding C, Zhu A, Tian Y (2014) Functional surface engineering of c-dots for fluorescent biosensing and in vivo bioimaging. *Acc Chem Res* 47(1): 20–30. <http://www.ncbi.nlm.nih.gov/pubmed/23911118>
- Ellerbee AK et al (2009) Quantifying colorimetric assays in paper-based microfluidic devices by measuring the transmission of light through paper. *Anal Chem* 81(20):8447–8452. doi:10.1021/ac901307q
- Fenton EM, Mascarenas MR, López GP, Sibbett SS (2009) Multiplex lateral-flow test strips fabricated by two-dimensional shaping. *ACS Appl Mater Interfaces* 1(1):124–129. doi:10.1021/am800043z
- Fiebig EW et al (2003) Dynamics of HIV Viremia and antibody seroconversion in plasma donors: implications for diagnosis and staging of primary HIV infection. *AIDS* 17(13):1871–1879. <http://www.ncbi.nlm.nih.gov/pubmed/12960819>
- Fluorescence Polarization (2010) <https://www.thermofisher.com/in/en/home/references/molecular-probes-the-handbook/technical-notes-and-product-highlights/fluorescence-polarization-fp.html>
- Ge L et al (2012) 3D Origami-based multifunction-integrated immunodevice: low-cost and multiplexed sandwich chemiluminescence immunoassay on microfluidic paper-based analytical

- device. *Lab Chip* 12(17): 3150–58. <http://www.ncbi.nlm.nih.gov/pubmed/22763468>
- Heiat M et al (2014) Surface engineering of solid supports; cellulose, nitrocellulose and nylon to increase the efficiency of antibody immobilization in diagnostic systems. *Int J Sci Eng Res* 5(1):1808–1814
- Hsu P-C, Chang H-T (2012) Synthesis of high-quality carbon nanodots from hydrophilic compounds: role of functional groups. *Chem Commun (Camb)* 48(33): 3984–3986. <http://www.ncbi.nlm.nih.gov/pubmed/22422194>
- Hu M (2013) Preparation method of carbon quantum dot test paper strip for detecting P24 antigen. <http://www.google.com/patents/CN103344756A?cl=en>
- Infectious Diseases (2016) <http://www.smartglobalhealth.org/issues/entry/infectious-diseases>
- Jeong S-G et al (2015) Toward instrument-free digital measurements: a three-dimensional microfluidic device fabricated in a single sheet of paper by double-sided printing and lamination. *Lab Chip* 15(4): 1188–94. <http://xlink.rsc.org/?DOI=C4LC01382D>
- Kim D, Herr AE (2013) Protein immobilization techniques for microfluidic assays. *Biomicrofluidics* 7(4):041501. doi:10.1063/1.4816934
- Lab on Paper (2008) *Lab on a Chip* 8(12): 1988. <http://xlink.rsc.org/?DOI=b814043j>
- Lea WA, Simeonov A (2011) Fluorescence polarization assays in small molecule screening. *Expert Opin Drug Discov* 6(1):17–32. doi:10.1517/17460441.2011.537322
- Lequin RM (2005) Enzyme immunoassay (EIA)/enzyme-linked immunosorbent assay (ELISA). *Clin Chem* 51(12): 2415–18. <http://www.ncbi.nlm.nih.gov/pubmed/16179424>
- Li H, Kang Z, Liu Y, Lee S-T (2012) Carbon nanodots: synthesis, properties and applications. *J Mater Chem* 22(46): 24230. <http://xlink.rsc.org/?DOI=c2jm34690g>
- Liang Q et al (2013) Easy synthesis of highly fluorescent carbon quantum dots from gelatin and their luminescent properties and applications. *Carbon* 60:421–428. doi:10.1016/j.carbon.2013.04.055
- Lim SY, Shen W, Gao Z (2015) Carbon quantum dots and their applications. *Chem Soc Rev* 44(1):362–381
- Liu J et al (2014) Development of a microchip europium nanoparticle immunoassay for sensitive point-of-care HIV detection. *Biosens Bioelectron* 61: 177–83. <http://www.ncbi.nlm.nih.gov/pubmed/24880655>
- Lu Y, Shi W, Qin J, Lin B (2010) Fabrication and characterization of paper-based microfluidics prepared in nitrocellulose membrane by wax printing. *Anal Chem* 82(1):329–335. doi:10.1021/ac9020193
- Ma S, Tang Y, Liu J, Jianmin W (2014) Visible paper chip immunoassay for rapid determination of bacteria in water distribution system. *Talanta* 120:135–140. doi:10.1016/j.talanta.2013.12.007
- Martinez AW, Phillips ST, Butte MJ, Whitesides GM (2007) Patterned paper as a platform for inexpensive, low-volume, portable bioassays. *Ange Chem Int Ed* 46:1318–1320
- Martinez AW, Phillips ST, Whitesides GM, Carrilho E (2010) Diagnostics for the developing world: microfluidic paper-based analytical devices. *Anal Chem* 82(1):3–10
- Moore RD, Chaisson RE (1999) Natural history of HIV infection in the era of combination antiretroviral therapy. *AIDS* 13(14): 1933–1942. <http://www.ncbi.nlm.nih.gov/pubmed/10513653>
- Mu X et al (2014) Multiplex microfluidic paper-based immunoassay for the diagnosis of hepatitis C virus infection. *Anal Chem* 86:5338–5344
- Pelton R (2009) Bioactive paper provides a low-cost platform for diagnostics. *Trends Anal Chem* 28(8):925–942. doi:10.1016/j.trac.2009.05.005
- Peng H, Travas-Sejdic J (2009) Simple aqueous solution route to luminescent carbonogenic dots from carbohydrates. *Chem Mater* 21(23):5563–5565. doi:10.1021/cm901593y
- Resch-Genger U et al (2008) Quantum dots versus organic dyes as fluorescent labels. *Nat Methods* 5(9): 763–75. <http://www.ncbi.nlm.nih.gov/pubmed/18756197>
- Rowland SP (1977) Cellulose: pores, internal surfaces, and the water interface, pp 20–45. doi:10.1021/bk-1977-0049.ch002
- Roy P et al (2015) Photoluminescent carbon nanodots: synthesis, physicochemical properties and analytical applications. *Mater Today* 18(8): 447–58. <http://linkinghub.elsevier.com/retrieve/pii/S1369702115001212>
- Samyn P (2013) Wetting and hydrophobic modification of cellulose surfaces for paper applications. *J Mater Sci* 48(19):6455–6498. doi:10.1007/s10853-013-7519-y
- Schüpbach J et al (1996) Heat-mediated immune complex dissociation and enzyme-linked immunosorbent assay signal amplification render p24 antigen detection in plasma as sensitive as HIV-1 RNA detection by polymerase chain reaction. *AIDS* 10(10): 1085–1090. <http://www.ncbi.nlm.nih.gov/pubmed/8874624>
- Sherman GG, Matsebula TC, Jones SA (2005) Is early HIV testing of infants in poorly resourced prevention of mother to child transmission programmes unaffordable? *Trop Med Int Health* 10(11):1108–1113
- Shi H et al (2014) Fluorescent carbon dots for biolmaging and biosensing applications. *J Biomed Nanotechnol* 10(10): 2677–99. <http://www.ncbi.nlm.nih.gov/pubmed/25992414>
- Sutthent R et al (2003) p24 antigen detection assay modified with a booster step for diagnosis and monitoring of human immunodeficiency virus type 1 infection. *J Clin Microbiol* 41(3): 1016–1022. <http://www.ncbi.nlm.nih.gov/pubmed/150255>
- Tang S, Hewlett I (2010) Nanoparticle-based immunoassays for sensitive and early detection of HIV-1 capsid (p24) antigen. *J Infect Dis* 201(Suppl 1): S59–S64. <http://www.pubmedcentral.nih.gov/articlerender.fcgi?artid=2943740&tool=pmcentrez&rendertype=abstract>
- Tenda K et al (2016) High-resolution microfluidic paper-based analytical devices for sub-microliter sample analysis. *Micromachines* 7(5): 80. <http://www.mdpi.com/2072-666X/7/5/80>
- Walling MA, Novak JA, Shepard JRE (2009) Quantum dots for live cell and in vivo imaging. *Int J Mol Sci* 10(2): 441–491. <http://www.mdpi.com/1422-0067/10/2/441/>
- Which Western Blot Detection Method Should You Use? (2012) <http://www.licor.com/bio/blog/western-blotting-2/western-blot-detection-method-fluorescence-chemiluminescence-and-colorimetric>
- Wu Y et al (2015) Development of a carbon dot (C-Dot)-linked immunosorbent assay for the detection of human α -fetoprotein. *Anal Chem* 87(16):8510–8516. doi:10.1021/acs.analchem.5b02019
- Zang D et al (2012) Electrochemical immunoassay on a 3d microfluidic paper-based device. *Chem Commun* 48(39):4683
- Zhao W, van den Berg A (2008) Lab on paper. *Lab on a Chip* 8(12): 1988. <http://xlink.rsc.org/?DOI=b814043j>
- Zhao W et al (2008) Paper-based bioassays using gold nanoparticle colorimetric probes. *Anal Chem* 80(22):8431–8437. doi:10.1021/ac801008q
- Zhu C, Zhai J, Dong S (2012) Bifunctional fluorescent carbon nanodots: green synthesis via soy milk and application as metal-free electrocatalysts for oxygen reduction. *Chem Commun* 48(75): 9367. <http://xlink.rsc.org/?DOI=c2cc33844k>
- Zhu S et al (2013) Highly photoluminescent carbon dots for multicolor patterning, sensors, and bioimaging. *Ange Chem Int Ed* 52(14):3953–3957
- Zuo J et al (2015) Preparation and application of fluorescent carbon dots. *J Nanomater* 2015: 1–13. <http://www.hindawi.com/journals/jnm/2015/787862/>